Journal Pre-proofs

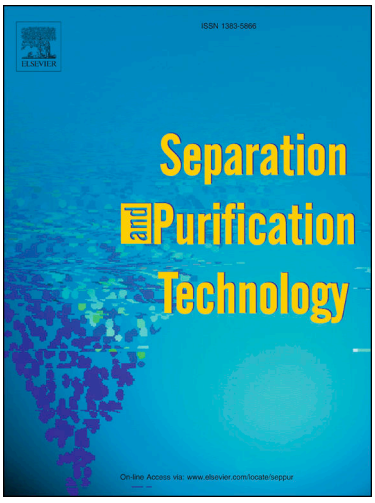

Purification of mercury-contaminated water using new AM-11 and AM-14 microporous silicates

Elaine Fabre, Arany Rocha, Simão P. Cardoso, Paula Brandão, Carlos Vale, Cláudia B. Lopes, Eduarda Pereira, Carlos M. Silva

PII: S1383-5866(19)34363-1
DOI: https://doi.org/10.1016/j.seppur.2019.116438
Reference: SEPPUR 116438

To appear in: *Separation and Purification Technology*

Received Date: 25 September 2019
Revised Date: 9 December 2019
Accepted Date: 15 December 2019

Please cite this article as: E. Fabre, A. Rocha, S.P. Cardoso, P. Brandão, C. Vale, C.B. Lopes, E. Pereira, C.M. Silva, Purification of mercury-contaminated water using new AM-11 and AM-14 microporous silicates, *Separation and Purification Technology* (2019), doi: https://doi.org/10.1016/j.seppur.2019.116438

Purification of mercury-contaminated water using new AM-11 and AM-14 microporous silicates

Elaine Fabre[a], Arany Rocha[b], Simão P. Cardoso[c], Paula Brandão[d], Carlos Vale[e], Cláudia B. Lopes[f], Eduarda Pereira[g]*, Carlos M. Silva[h]*

[a] CICECO, CESAM, Universidade de Aveiro, Portugal (elainefabre@ua.pt)

[b] CICECO, Universidade de Aveiro, Portugal (silvaldinorocha@ua.pt)

[c] CICECO, Universidade de Aveiro, Portugal (simaocardoso@ua.pt)

[d] CICECO, Universidade de Aveiro, Portugal (pbrandao@ua.pt)

[e] CIIMAR, Universidade do Porto, Portugal (carlos.vale@ciimar.up.pt)

[f] CICECO, Universidade de Aveiro, Portugal (claudia.b.lopes@ua.pt)

[g] CESAM & LAQV-REQUIMTE, Universidade de Aveiro, Portugal (eduper@ua.pt)

[h] CICECO, Universidade de Aveiro, Portugal (carlos.manuel@ua.pt)

* Corresponding authors: Eduarda Pereira (eduper@ua.pt) and Carlos M. Silva (carlos.manuel@ua.pt)

ABSTRACT

Water is an essential resource on Earth and the maintenance of its quality led to the incentive of water reuse programmes. Among the most relevant contaminants, mercury is recognized for its toxicity and biomagnifications along the food chain, reason why its removal from aqueous solutions was studied in this essay using two microporous materials for the first time. The ability of a niobium silicate, called AM-11 (Aveiro-Manchester No 11), and of a vanadium silicate, AM-14 (Aveiro-Manchester No 14), were assessed under batch conditions, at fixed temperature and pH. These microporous materials were synthesized and characterized by SEM, PXRD, ICP-OES, TGA and elemental analysis. Because of their excellent ion exchange properties, equilibrium and

kinetics assays were performed using only a few mg dm^{-3} of material. The most relevant two- and three-parameter isotherms were used to fit the experimental data. Langmuir isotherm adjusted better the AM-11 data (deviation of 3.58 %, R^2_{adj}=0.980, AIC=52.8), predicting a maximum uptake of 161 mg g^{-1}, while the AM-14 data were better fitted by the Temkin model (deviation of 3.92 %, R^2_{adj}=0.985, AIC=54.2). The kinetic study was performed using Elovich, pseudo-first order and pseudo-second order models. The pseudo–second order and Elovich equations provided the best fits for both materials. The Elovich equation achieved a better correlation in the initial branch while the pseudo-second order expression was more efficient for the horizontal branch. The intraparticle diffusivities of counter ions were also assessed using a kinetic model based on the Nernst-Plankequations. Performance of these two microporous materials to remove mercury has been compared with other sorbents, highlighting their potential as ion exchangers.

Keywords: AM-11; AM-14; ion exchange; mercury removal; modelling; water treatment

1. Introduction

The contamination of waters and aquatic systems due to the discharge of toxic elements has caused worldwide concern for the last years, due to their well-known effects on biota and human health [1,2]. Several industries are responsible for the discharge of metals into the aquatic system including the production of lamps, batteries, electronic devices, chlor-alkali production and petroleum refining [3]. Mercury is considered one of the most hazardous non-essential metals, occupying the third position in the rank of the most dangerous substances of the Agency for Toxic Substances & Disease Registry (ATSDR), which is elaborated based on a combination of its environmental frequency, toxicity, and potential for human exposure ("Substance Priority List | ATSDR"). Mercury dangerousness is due to its persistent character, ease of accumulation and amplification along the food chain causing a lot of toxic effects on living organisms [5–7]. Therefore, its removal from water and wastewaters is a key issue in water remediation technologies and that is not a trivial task. The study of Hg removal is delicate and the efficiency of the process is highly dependent on the speciation, transformation and reactivity of Hg(II) species in waters [8]. In fresh waters the interactions between Hg(II) and the dissolved organic matters strongly influence its removal due to the high thermodynamic stability of the organic mercury complexes formed, which are several orders of magnitude higher than non-sulfidic mercury complexes [8,9].

A variety of processes are available for the treatment of aqueous streams contaminated with toxic metals. The most important are electrochemical techniques, chemical precipitation, membrane processes, flotation, solvent extraction, ion exchange and adsorption [10–16]. However, many of these methods exhibit high operating and maintenance costs, difficult sludge disposal and are non-effective to treat water with low metal concentrations [2,6,17]. Comparatively, the ion exchange is widely used in industry, because of its simple operation and efficiency to treat large volumes of dilute solutions [6,18,19]. Here, the need for low cost,

accessible and recoverable sorbents guides the research and development of new materials to replace the ion exchange resins largely used [6,20].

Zeolites and other zeolite-type materials are receiving special attention in ion exchange processes due to their structure, high surface areas and selectivity, which provide good cost-benefit ratios [21–24]. The negative charge of the porous framework of these materials is balanced by the presence of exchangeable cations electrostatically held within their channels and/or cavities, which makes them adequate for cationic exchange [25]. Despite the great interest in ion exchange using microporous materials, only a few publications have addressed realistic and low concentrated solutions. Recently, titanium silicates, displaying zeolite-type properties, have attracted much interest [26]. Materials like ETS-4 and ETS-10 have been used for Hg(II) and Cd(II) removal from diluted aqueous solutions and these materials have been proposed as good exchangers [6,12,19,27,28]. As an extension of these works, novel microporous niobium and vanadium silicates have been synthesized and studied here for Hg(II) removal, namely, AM-11 (Aveiro-Manchester microporous solid no. 11), as an example of a niobium silicate, and AM-14 (Aveiro-Manchester microporous solid no. 14), as an example of vanadium silicate [29,30]. The crystal structure of AM-11 and AM-14 materials are still unknown. Nevertheless, from a wide range of characterisation techniques one may say that both materials exhibit three-dimensional network of interconnected channels, composed by tetrahedral SiO_4 units and octahedral Nb^{5+} atoms for AM-11 [31] and V^{4+} for AM-14 [30]. The pore size of these two silicates were accessed by adsorption isotherms of different organic molecules (n-hexane, benzene, tripropylamine) indicating that AM-11 contains medium pore size of 4 Å and AM-14 possess a median pore size of 6.8 Å [29,30]. The NH_4^+ ions are the counter ions used to balance the charge associated with niobium framework [31] and its theoretical capacity is 2.12 meq g^{-1}, while in the case of AM-14 the Na^+ cations are the neutralizing species and its theoretical capacity is 5.20 meq g^{-1} [30].

Taking into account the small pore diameters mentioned above for AM-11 and AM-14 (4 Å and 6.8 Å, respectively) along with the strong and long-range nature of the electrostatic interactions, and the Donan exclusion principle (*i.e.,* solution co-ions cannot penetrate the zeolite materials), the diffusing species never escape from the force field of the solid matrix and thus the sorption mechanism of mercury is ion exchange. Accordingly, the systems of interest in this work are Hg(II)/AM-11 and Hg(II)/AM-14.

In line with one of the goals of 2030 Agenda for Sustainable Development of United Nations, which includes improving water quality by reducing pollution, minimizing the presence of hazardous chemicals, and to substantially increase water recycling and safe reuse, here we investigate the applicability of AM-11 and AM-14 to remove Hg(II) from diluted solutions, prospecting their potential for treating contaminated waters and industrial effluents. Batch experiments were carried out for two systems (Hg(II)/AM-11 and Hg(II)/AM-14), for which the kinetics and equilibrium were investigated experimentally and theoretically by applying well-known kinetic equations and isotherms. To the best of our knowledge these microporous materials have never been applied in ion exchange processes. With this study, we intend to contribute to the better knowledge of Hg(II) removal process, searching alternative materials for improving water quality and contributing to sustainable development goals of United Nations.

2. Materials and methods

2.1. Chemicals

All reagents used in this work were of analytical grade. They were purchased and used without additional purification. The certified standard solution of mercury(II) nitrate (1000 ±2 mg dm^{-3}), the sodium hydroxide (≥ 99 %), the ammonia solution (25 %), the sodium silicate solution (≥ 25 %) and the vanadium(IV) oxide sulfate hydrate (≥ 99 %) were purchased from

Merck. The tetraethyl orthosilicate (≥ 99 %), sodium chloride (≥ 99 %), and niobium chloride (≥ 99 %), were acquired from Aldrich. All working solutions, including standards for the calibration curves, were obtained by dissolving or diluting the corresponding stock solution in high purity water (18.2 MΩ cm^{-1}, Milli-Q system).

2.2. Sorbents materials

2.2.1. Synthesis

AM-11 and AM-14 were studied for Hg(II) removal from aqueous solution. The AM-11 sample used in this work was prepared using NH^{4+} as cation. Briefly, AM-11 was synthesized as follows: a solution was made by mixing 0.193 g of $NbCl_5$, with 3 cm^3 of HCl (37 %). A second solution was made by mixing 4 cm^3 of H_2O and 1.28 g of tetraethyl orthosilicate. These two solutions were combined and stirred thoroughly, then 50 cm^3 of ammonium solution (25 %) was added. The gel was autoclaved for 15 days at 200 °C. The resulting crystalline product was filtered off, washed with distilled water and then dried at room temperature The final product obtained was an off-white microcrystalline powder [29].

The synthesis of AM-14 started with an alkaline solution, by dissolving 5.02 g of sodium silicate solution, 9.05 g of H_2O, 0.540 g of NaOH and 0.760 g of NaCl. A second solution was prepared by mixing 6.66 g of H_2O with 1.44 g of $VOSO_4 \cdot 5H_2O$. The AM-14 gel was autoclaved for 3 days at 230 °C. The crystalline green powder was filtered out, washed and dried at room temperature [30].

2.2.2. Structural and chemical characterization

The crystal morphology of AM-11 and AM-14 was analysed using scanning electron microscopy (SEM) on a Hitachi SU-70 SEM microscope with a Bruker Quantax 400 detector operating at 20 kV. The powder X-Ray diffraction (PXRD) patterns of both samples were recorded

on an Empyrean PANalytical diffractometer equipped with a Cu-Kα monochromatic radiation source. Inductively coupled plasma optical emission spectroscopy (ICP-OES) analyses (for Si, Nb, V and Na) were carried out on a Horiba Jobin Yvon Activa M spectrometer (detection limit of *ca.* 20 μg dm^{-3}; experimental range of error of *ca.* 5 %). Elemental analysis of nitrogen present in AM-11 sample was performed using a Truspec 630-200-200 instrument. Thermogravimetric analysis curves were measured with Shimadzu TGA-50. The heating rate was 10 °C min^{-1} from room temperature until 800 °C for AM-11 and until 700 °C for AM-14. The point zero charge (PZC) of AM-11 was determined according to an adaptation of the immersion method proposed by Fiol and Villaescusa [65] using an incubator shaker HWY-200D and the solution pH was measured on a WTW series 720 meter. In the case of AM-14, the measurement was not performed over all pH range (0-9) as in the case of AM-11, due to material stability.

2.3. Batch experiments

All the material was washed before the experiments with nitric acid 25 % for 24 hours and then plenty rinsed with ultra-pure water. The ability of niobium and vanadium silicates to sorb Hg(II) from solution was assessed by contacting each microporous material with solutions of fixed concentration for a determined period of time. All assays were performed in batch conditions, at 22±1 °C in 1 dm^3 volumetric flasks magnetically stirred at 500 rpm. The Hg(II) solutions were prepared diluting the standard solution in high purity water (18.2 MΩ cm^{-1}) to the desired initial concentration (1 mg dm^{-3}). The pH of the solutions was adjusted to 6 with 0.1 mol dm^{-3} NaOH. A blank experiment (without the niobium or vanadium silicate) was always run as control under the same operating conditions. Rigorous masses of AM-11 or AM-14 were added to the previous aqueous solutions and this moment was considered the initial time of the experiment. Solution samples were withdrawn at increasing times, filtered with a Millipore membrane of 0.45 μm, adjusted to pH < 2 with HNO_3 and immediately analysed afterwards. The

concentration of Hg(II) in the samples was measured using a cold vapour atomic fluorescence spectroscope (CV-AFS), on a PSA cold vapour generator (model 10.003) coupled to a Merlin PSA detector (model 10.023). The liquid samples containing mercury were introduced in the equipment, the Hg(II) was reduced by $SnCl_2$ to its elemental form and quantified in the detector. The response was obtained as a signal and converted to concentration through a calibration curve.

For AM-11, twelve experiments were accomplished: ten to determine equilibrium points and two to measure kinetic removal curves (in this case, the final points were also used to get additional equilibrium data). For AM-14, eleven experiments were carried out: nine to obtain isotherm points, and the remaining two to generate removal curves (and also two extra equilibrium data). The detailed experimental conditions can be found in Table 1.

Table 1. Experimental conditions studied: Temperature = 22±1 °C, solution volume = 1 dm^3, initial Hg(II) concentration = 1 mg dm^{-3}, pH 6.

No. Exp. for AM-11	**1**	**2**	**3**	**4**	**5**	**6**	**7**	**8**	**9**	**10**	**11**	**12**
Mass of AM-11 (mg)	1.0	1.5	2.5	3.7	5.1	6.0	7.0	8.0	10.0	12.1	6.5	14.0
Data measured	Equilibrium										Kinetic and equilibrium	
No. Exp. for AM-14	**13**	**14**	**15**	**16**	**17**	**18**	**19**	**20**	**21**	**22**		**23**
Mass of AM-14 (mg)	1.5	2.0	2.5	3.0	3.8	4.0	5.0	10.0	12.0	6.5		3.5
Data measured	Equilibrium									Kinetic and Equilibrium		Kinetic

The average amount of sorbed Hg(II) per unit mass of microporous material, q_A (mg g^{-1}), was calculated by material balance to the whole system at time t:

$$q_A = \frac{V_L}{m_S}(C_{A0} - C_A) \quad (1)$$

where subscript A denotes mercury(II), V_{L} (dm^3) is the solution volume, m_{S} (g) is the mass of AM-11 or AM-14, C_{A0} (mg dm^{-3}) is the initial concentration of Hg(II) in solution, and C_{A} (mg dm^{-3}) is its concentration at any time t.

2.4. Kinetic and equilibrium modelling

2.4.1. Kinetic models

The kinetics of Hg(II) ion exchange on AM-11 and AM-14 was experimentally studied by batch ion exchange assays. Kinetic data depend on the chemical and structural properties of the materials, stirring velocity, and the inherent transport properties of the system. The pursue of sorption elucidate the viability of the ion exchange process to remove contaminants [33].

Ion exchange is essentially a diffusion process subject to a stoichiometric restriction, therefore its rate depends on the mobilities of both counter ions. This process is distinct from a chemical reaction in the usual sense, though some simple empirical or semi-empirical expressions, which were initially derived for adsorption considering the process as a chemical reaction, are frequently adopted to fit ion exchange kinetic data with the aim to evaluate the behaviour of the process. One may cite, for instance, the pseudo-first order (PFO), pseudo-second order (PSO) and Elovich equations. Accordingly, the significance of the intrinsic parameters has little in common with the rate constants of chemical reactions [34]. Phenomenological principles-based models should be preferred in order to obtain theoretically consistent information about the process. Rodrigues and Silva [35] compared the PFO equation with the linear driving force model of Glueckauf, and demonstrated that the kinetic constants of both models showed relevant differences mainly in their temperature dependence. Nonetheless, in the case of linear isothermal conditions the two models are formally equivalent. In this work, the above mentioned models were applied to fit the experimental data and extract information about the Hg(II) removal from aqueous solutions.

The PFO equation of Lagergren [36,37] assumes that the uptake kinetics is proportional to the distance to the final equilibrium concentration:

$$\frac{dq_A}{dt} = k_1(q_{Ae} - q_A) \quad (2)$$

where k_1 (h^{-1}) is a rate constant, q_{Ae} (mg g^{-1}) is the concentration of sorbed metal at final equilibrium, and t (h) is time. After integration from the initial clean particle condition ($t = 0$, $q_A = 0$) to any time t and solid loading q_A, one obtains:

$$\ln (q_{Ae} - q_A) = \ln q_{Ae} - k_1 t \quad (3)$$

The PSO model [38] can also be applied to represent the ion exchange kinetics along time. Its corresponding differential and integrated expressions embody a rate constant (k_2, g mg^{-1} h^{-1}) and are given by:

$$\frac{dq_A}{dt} = k_2(q_{Ae} - q_A)^2 \quad (4)$$

$$\frac{t}{q_A} = \frac{1}{k_2 q_{Ae}^2} + \frac{1}{q_{Ae}} t \quad (5)$$

The Elovich equation [39,40] describes the sorption kinetics on heterogeneous surfaces, and it is represented by:

$$\frac{dq_A}{dt} = \alpha e^{-\beta q_A} \quad (6)$$

$$q_A = \frac{1}{\beta} \ln (\alpha\beta) + \frac{1}{\beta} \ln t \quad (7)$$

where α is the initial sorption rate (mg g^{-1} h^{-1}) and β (g mg^{-1}) is the desorption constant.

With the objective to estimate the intraparticle diffusion coefficient of the counter ions of interest, a phenomenological model based on the kinetic equations of Nernst-Plankformalism [25,34,66,67] has also been included in the calculations.

2.4.2. Equilibrium Isotherm models

The study of equilibrium is essential for evaluating the viability of sorption processes. Relevant properties and the affinity of the ion exchange system can be disclosed by isotherms, being important for the effective design of metal removal process [40]. The most relevant two-parameter isotherms (Langmuir, Freundlich, Temkin and Dubinin-Radushkevich) and three-parameter isotherms (Langmuir-Freundlich, Redlich-Peterson and Toth) were selected in this essay to represent the experimental data.

Langmuir Isotherm. This is the most known isotherm and assumes that the sorbent contains a finite number of equivalent active sites, the sorption energy is uniform, the sorbed phase is ideal and forms a monolayer at solid surface [41,42]. It is given by:

$$q_{\mathrm{Ae}} = \frac{q_{\mathrm{m,L}} K_{\mathrm{L}} C_{\mathrm{Ae}}}{1 + K_{\mathrm{L}} C_{\mathrm{Ae}}} \tag{8}$$

where $q_{\mathrm{m,L}}$ (mg g^{-1}) is the sorption capacity, related with monolayer coverage, and K_{L} (dm^3 mg^{-1}) is the Langmuir equilibrium constant.

Freundlich Isotherm. This equation is applied to non-ideal systems, with heterogeneous surfaces and multilayer sorption, and assumes an exponentially decaying function of site density with respect to the sorption energy [40,43]:

$$q_{\mathrm{Ae}} = K_{\mathrm{F}} C_{\mathrm{Ae}}^{1/n_{\mathrm{F}}} \tag{9}$$

Here, K_{F} (mg$^{1-1/n_{\mathrm{F}}}$ dm$^{3/n_{\mathrm{F}}}$ g^{-1}) and n_{F} are the Freundlich constants. The parameter n_{F} is related with the nonlinearity of the model: the larger is this value, more nonlinear is the isotherm [44]. One limitation of Freundlich model is that under extremely low concentrations it does not recover the Henry's law, which would be expected in advance.

Temkin Isotherm. This equation assumes that the heat of sorption, E_θ, decreases linearly with fractional coverage θ [45]. As in the case of Freundlich isotherm, it does not exhibit a finite saturation limit [44]. It is mathematically given by:

$$\theta = \frac{RT}{\Delta E} ln(AC_{\mathrm{Ae}}) \tag{10}$$

where ΔE (J mol^{-1}) represents the variation of the heats of sorption corresponding to the particle initially free of solute ($\theta = 0$) and at maximum coverage ($\theta = 1$), $R = 8.314$ J mol^{-1} K^{-1} is the ideal gas constant, T (K) is the absolute temperature, and A (dm^3 mg^{-1}) is the isotherm equilibrium binding constant. Setting $B = q_{\mathrm{m,T}} RT/\Delta E$ (mg g^{-1}), the equation is rewritten as:

$$q_{\mathrm{Ae}} = B ln(AC_{\mathrm{Ae}}) \tag{11}$$

Dubinin-Radushkevich Isotherm. This equation was originally developed for adsorption and is based on the potential theory of Polanyi [46]. The process relies on the micropore volume filling concept instead of a layer-by-layer adsorption onto pore walls, and takes into account the energetic heterogeneity of the solid and the interactions between sorbed species [47–50] It is frequently extended to ion exchange equilibrium [51,52]. The isotherm is described by:

$$q_{\mathrm{Ae}} = q_{\mathrm{m,DR}} e^{-B_{\mathrm{DR}} \varepsilon^2} \tag{12}$$

$$\varepsilon = RT \ln\left[1 + \frac{1}{\mathrm{C_{Ae}}}\right] \quad \text{and} \quad E = \left[\frac{1}{\sqrt{2B_{\mathrm{DR}}}}\right] \tag{13}$$

where $q_{\mathrm{m,DR}}$ (mg g^{-1}) is the solid capacity, B_{DR} (mol^2 J^{-2}) is the Dubinin-Radushkevich constant, ε (J mol^{-1}) is the Polanyi potential**.** The magnitude of E represents the free energy change when 1 mol of solute is transferred to the surface of the solid and may be used to distinguish the sorption mechanisms**.**

Langmuir-Freundlich isotherm. At low concentrations, this three-parameter isotherm is essentially the Freundlich isotherm and, at high sorbate concentrations, it predicts a monolayer

sorption characteristic of Langmuir model [40,53]. The Langmuir-Freundlich equation is given by:

$$q_{\mathrm{Ae}} = \frac{q_{\mathrm{m,LF}}(K_{\mathrm{LF}}C_{\mathrm{Ae}})^{n_{\mathrm{LF}}}}{1 + (K_{\mathrm{LF}}C_{\mathrm{Ae}})^{n_{\mathrm{LF}}}} \quad (14)$$

where $q_{\mathrm{m,LF}}$ (mg g^{-1}) is the capacity of the material, K_{LF}(dm^3 mg^{-1})$^{n_{\mathrm{LF}}}$ is the Langmuir-Freundlich constant, and n_{LF} is the heterogeneity index, which varies from 0 to 1. If the material is homogeneous, n_{LF} is assumed to be 1, if the material is heterogeneous, n_{LF} gets values lower than 1 [54].

Redlich-Peterson Isotherm. This model embodies characteristics of both Langmuir and Freundlich isotherms [40]. It can be expressed as follows:

$$q_{\mathrm{Ae}} = \frac{K_{\mathrm{RP}}C_{\mathrm{Ae}}}{1 + a_{\mathrm{RP}}C_{\mathrm{Ae}}^{n_{\mathrm{RP}}}} \quad (15)$$

where K_{RP} (dm^3 g^{-1}) and a_{RP} (dm^3 mg^{-1})$^{n_{\mathrm{RP}}}$ are the Redlich-Peterson constants, and n_{RP} is the isotherm exponent. At low concentrations the Henry's law is recovered and at high concentrations it approaches Freundlich behaviour [40].

Toth Isotherm. This model is derived considering the potential theory and it is applicable to heterogeneous sorption. It assumes a quasi-Gaussian energy distribution and most sites exhibits sorption energies lower than the mean value [40,55]. It is represented by the following equation:

$$q_{\mathrm{Ae}} = \frac{q_{\mathrm{m,Th}}C_{\mathrm{Ae}}}{(a_{\mathrm{Th}} + C_{\mathrm{Ae}}^{n_{\mathrm{Th}}})^{1/n_{\mathrm{Th}}}} \quad (16)$$

where $q_{\mathrm{m,Th}}$ (mg g^{-1}) is the solid capacity, a_{Th} (mg dm^{-3})$^{n_{\mathrm{Th}}}$ is the Toth isotherm constant, and n_{Th} the isotherm exponent.

2.4.3. Error analysis

All the parameters of the kinetic and equilibrium models were obtained by nonlinear regression using the Nelder-Mead simplex algorithm to minimize the error between calculated and experimental data. With the aim to find out the most suitable models, the coefficient of determination (R^2), the adjusted coefficient of determination (R^2_{adj}), the average absolute relative deviation ($AARD$), the sum of squares (SS), and the Akaike's Information Criterion (AIC) [56] were calculated. The corresponding definitions and mathematical expressions are given by:

$$R^2 = 1 - \frac{\sum(\hat{y_i} - y_i)^2}{\sum(y_i - \bar{y})^2} \quad (17)$$

$$R^2_{\text{adj}} = 1 - (1 - R^2)\frac{(N_{\text{DP}} - 1)}{(N_{\text{DP}} - N_{\text{P}} - 1)} \quad (18)$$

$$AARD(\%) = \frac{100}{N_{\text{DP}}}\sum_{i=1}^{N_{\text{DP}}} \frac{\left|\hat{y_i} - y_i\right|}{y_i} \quad (19)$$

$$SS = \sum(\hat{y_i} - y_i)^2 \quad (20)$$

$$AIC = N_{\text{DP}}\ln\left(\frac{SS}{N_{\text{DP}}}\right) + 2N_{\text{P}} + \frac{2N_{\text{P}}(N_{\text{P}} + 1)}{N_{\text{DP}} - N_{\text{P}} - 1} \quad (21)$$

where N_{DP} is the number of data points, N_{P} is the number of parameters, y_i and $\hat{y_i}$ are the experimental and calculated values for point i, respectively, and $\bar{y}$ is the average of all observed values. The value of AIC determines which model is more likely to be correct and quantifies how much more likely. The lower the AIC (on a scale from -∞ to +∞) the better is the model to describe the experimental data than the alternative models [56].

3. Results and discussion

3.1. Characterization of AM-11 and AM-14 microporous materials

Figure 1 shows the X-Ray diffractograms of the as-synthesized AM-11 and AM-14 used for the Hg(II) removal studies, revealing that they are identical to those published by Rocha *et*

al. [29] and Brandão *et al*. [30], respectively. SEM images presented in Figure 2 reveal that both microporous materials contain only a single phase: the AM-11 crystals are needles with *ca*. 10 µm in length and AM-14 consists of thin plates with size of *ca*. 1-2 µm. Table 2 shows the percentages of N, Si and Nb for AM-11, and of Na, Si and V for AM-14, as well as the main molar ratios. The molar ratio between Si and Nb in AM-11 is 4.5, and in AM-14 Si/V is 4, which are in accordance to the values published previously. The theoretical ion exchange in AM-14 is performed by 2 mol of Na for each mol of V, and in AM-11, according with the amount of nitrogen (Table 2), by one cation NH_4^+ for each Nb present. The TGA curves shown in Figures A1 and A2 (see Supplementary Material) were obtained under air for both materials. The curves reveal a gradual weight loss from room temperature until 800 °C for AM-11, and until 700 °C for AM-14. Total mass losses were 13 % (AM-11) and 14 % (AM-14), although only 4-5 % were observed below 100 °C, suggesting loss of adsorbed water. Losses at higher temperatures were most likely due to the release of water molecules strongly coordinated with the cations, which is related with the structure of the materials.

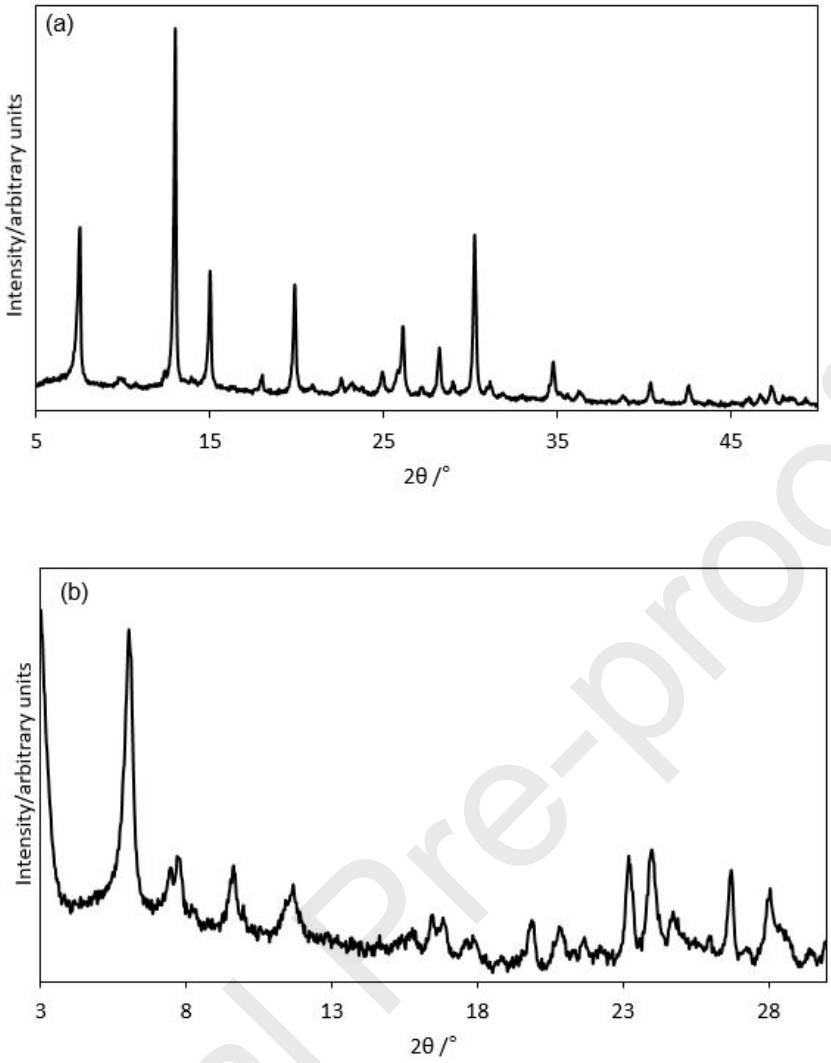

Figure 1. PXRD patterns of AM-11 (a) and AM-14 (b).

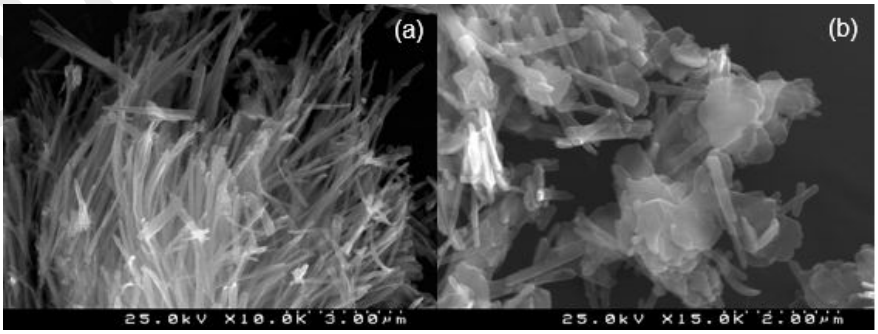

Figure 2. SEM images of AM-11 (a) and AM-14 (b)

Table 2 - Composition of AM-11 and AM-14

Material	Concentrations (wt.%)			Molar ratios (mol/mol)	
AM-11	N	Si	Nb	Si/Nb	N/Nb (mol/mol)
	2.7	23	17	4.5	1.0
AM-14	Na	Si	V	Si/V	Na/V
	8.7	27	10	4.0	2.0

The measurement of the Point of Zero Charge (PZC) of both materials was also considered (see Supplementary Material): in the case of AM-11, the characteristic |ΔpH| *versus* initial pH curve is always negative over pH range 0-9, which means the microporous silicate surface is negatively charged, with advantage for cation exchange (in this essay, pH was constant and equal to 6). In the case of AM-14 the same occurs at pH 6, *i.e.* surface is negatively charged, and similar conclusions may be drawn.

3.2. Removal of Hg(II) by AM-11 and AM-14 materials

The variation with time of the normalized Hg(II) concentration, for two masses of AM-11 and AM-14, is presented in Figure 3. During ion exchange, it is possible to distinguish two periods for the two quantities of materials. In the first 48 h the removal is faster than the slower subsequent period towards the equilibrium. This pattern mirrors the large driving force for mass transport at the beginning of the process, when particles are free of Hg(II) or contain negligible quantities of the metal.

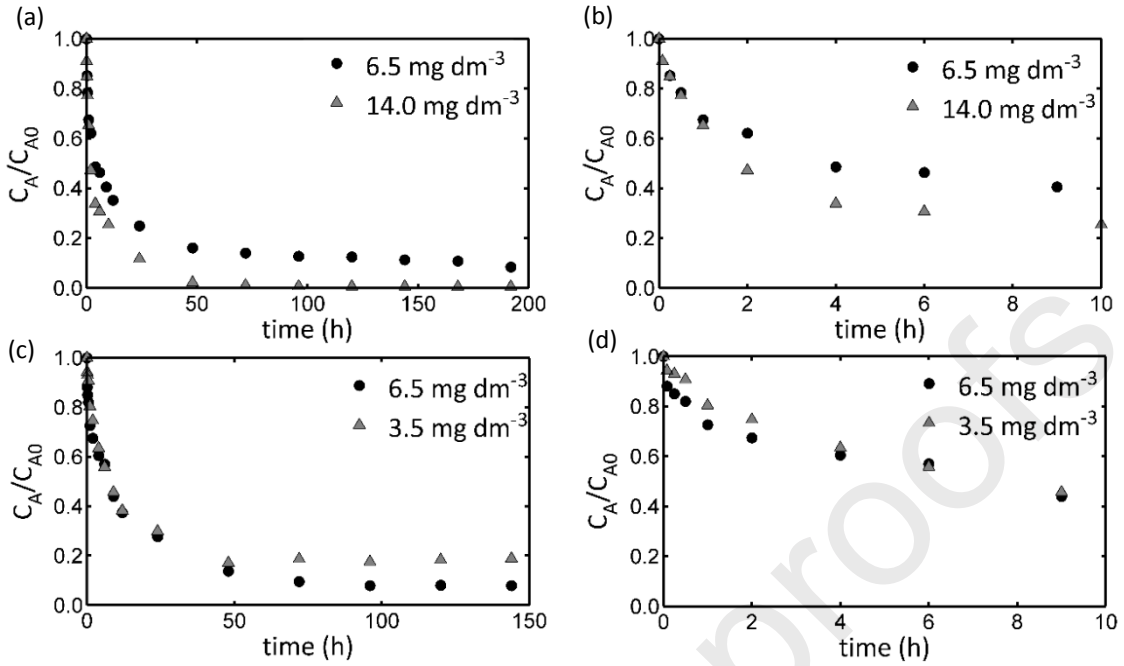

Figure 3. Normalized Hg(II) concentration in the liquid phase for AM-11 ((a) and (b)) and AM-14 ((c) and (d)); two quantities of sorbents were tested

Despite the differences between AM-11 and AM-14, the kinetic curves and the removal efficiencies of both materials towards Hg(II) are very similar under the same operating conditions. For instance, only 6.5 mg dm^{-3} of microporous materials were able to remove 92 % of the Hg(II) initially present in solution, reflecting the great ion exchange capacity of AM-11 and AM-14. Moreover, no relevant differences were observed on the kinetics of the two materials: the initial rates had the same order of magnitude (0.607 and 0.528 mg dm^{-3} h^{-1}, values calculated from the first derivate of $C_A = f(t)$ at $t = 0$), and the equilibrium time was approximately 96 h for both, although the dimensionless concentration in the case of AM-11 decreased smoothly until 192 h.

The experiments performed with two material doses emphasize the effect of mass on the removal process. Increasing the dose of AM-11 from 6.5 to 14.0 mg dm^{-3} led to an additional removal from 92 to 99 % of Hg(II) from solution, while the dose increment of AM-14 from 3.5 to 6.5 mg dm^{-3} resulted in the uptake of 81 to 92 % of the Hg(II) initially present in solution. These

results are naturally due to the fact that more mass provides additional sorption sites available for ion exchange. The equilibrium time was not very sensitive to the changes in the amount of material, although slightly small equilibrium time was found for the higher mass of AM-11. Both materials showed fast kinetics, even smaller masses being sufficient to remove more than 70 % of the Hg(II) in solution during the first 24 hours.

In Figure A4 (Supplementary Material) it is plotted the mercury speciation in aqueous solution for the experimental conditions of this essay, namely, initial metal concentration of 1 mg dm^{-3} and temperature of 22±1 °C. It is possible to conclude that mercury occurs as neutral ($Hg(OH)_2$) and positive ($[Hg(OH)]^+$ and Hg^{2+}) species, while complexes with NO_3^- are negligible and thus not represented. At pH 6 the predominant form is $Hg(OH)_2$ and no precipitation was detected. This fact implies that at particle surface the solution equilibrium is shifted to the mercury(II) form, and then ion exchange proceeds subjected to the already discussed steric and Donan restrictions.

The excellent performances of AM-11 and AM-14 obtained in this work are very promising for waters treatment, though real systems involve competitive ions that may interfere with the Hg(II) uptake. Nonetheless, studies in literature using zeolites report little or no impacts upon Hg(II) removal by the presence of competitive ions in solution [21,32]. Materials like ETS-10, ETS-4, AM-2 and AV-13 exhibited similar sorption efficiencies in seawater or in solutions containing $MgSO_4$ or NaCl [32]. Furthermore, the performances of the zeolites Ag-X, Na-A, Na-X, 13X and 4A for Hg(II) removal from an industrial wastewater were not penalized by the presence of foreign ions [21]. On the other hand, Hg(II) sorption using biosorbents, like *E. globulus* bark, decreased with increasing NaCl concentration in solution [57]. The same happened in the case of bracken ferns [58] but no influence was observed in the case of Hg(II) removal by banana peels [70]. In another study, the addition of NaCl and Cu(II) decreased Hg(II)

sorption using *Cystoseira baccat,* while the existence of Cd(II), Mg(II), Zn(II) and Ca(II) did not penalize Hg(II), and the presence of Pb(II) improved the biosorbent removal efficiency [59].

Desorption studies also need to be considered in order to reuse the synthetic materials and recover the sorbed metal if it is of interest. Depending on the easiness of desorption, the solid may be subsequently applied for several cycles as long as its efficiency, stability and structure are maintained [71]. For instance, in the particular case of mercury, its desorption from functionalized zeolite PPy/SH-Beta/MCM-41 using 0.5 M H_2SO_4 was able to recover more than 90 % of the metal. The efficiency of the sorbent was analysed during five cycles and it was possible to remove Hg(II) in all of them, although metal removal was decreasing along the cycles [72]. In a different work, Hg(II) was removed from aqueous solutions using titanosilicate ETS-4 in fixed-bed [68] and its regeneration was successfully accomplished with a concentration gradient (0.05–0.25 M) of EDTA-Na2 solution. The metal recovery was very fast and reached 98 % with a concentration factor of 920 (ratio between the maximum peak concentration during elution and the initial metal concentration). The utilization of $NaNO_3$ solutions (10^{-3} M) was also tested to guarantee the complete elution of Hg(II) and Cd(II) from loaded ETS-4 [69].

3.3. Modelling

The solid loadings along time were modelled by PFO, PSO and Elovich equations. The variation with time of the experimental and calculated Hg(II) concentrations in the materials are shown in Figures 4 and 5. The PSO and Elovich models show the best fit to the experimental data. The PSO model have presented good description of the kinetic data from other mercury removal processes reported in the literature [53,60]. In general, there is a good agreement between the Elovich fitting and the experimental q_{A} values for the ascend branch, while the PSO expression achieved a better performance on the horizontal branches of each curve. Moreover, the AARDs found for the microporous materials in the first 6 h were between 2.96 % and 8.18 %

for the Elovich model and between 12.1 % and 24.6 % for the PSO model, which confirms the above mentioned. The best fit parameters are shown in Table 3, and the values of the rate constants (k_1, k_2 and α) of the PFO, PSO and Elovich models follow the sorbent mass tendency, lower values for the smaller doses of material.

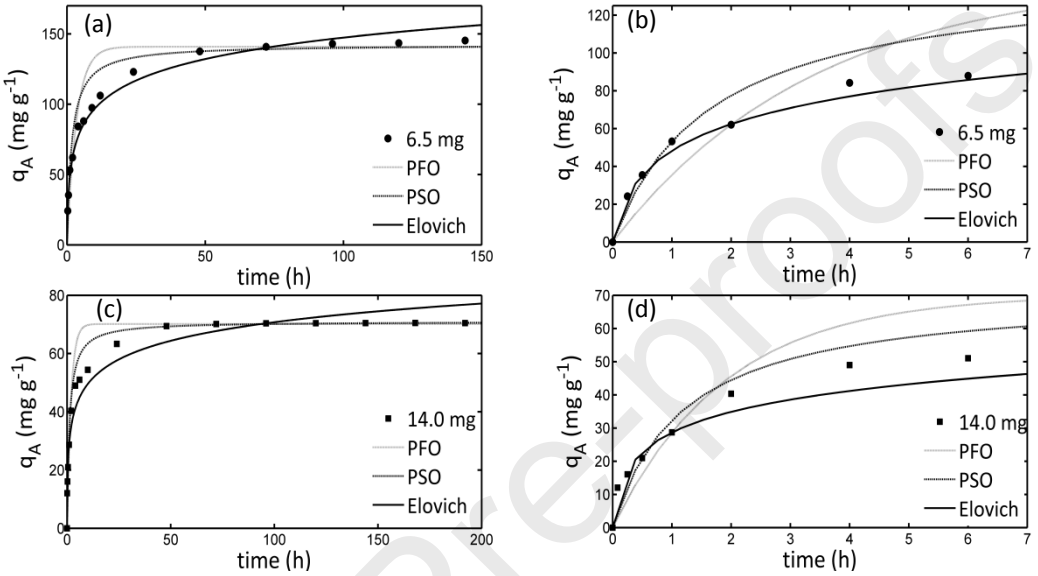

Figure 4. Sorption kinetics modelling for the AM-11 particles: (a) and (b) represent the sorbent dosage of 6.5 mg dm^{-3}, (c) and (d) represent the sorbent dosage of 14.0 mg dm^{-3}.

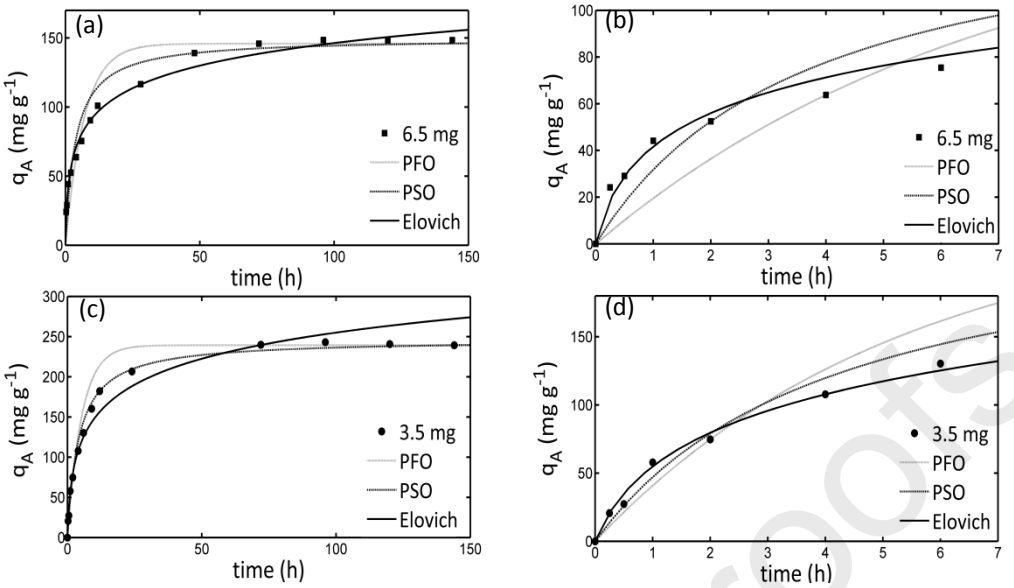

Figure 5. Sorption kinetics modelling on the AM-14 particles ((a) and (b) represent the sorbent dosage of 6.5 mg dm^{-3}, (c) and (d) represent the sorbent dosage of 3.5 mg dm^{-3}).

Table 3 – PFO, PSO and Elovich constants for Hg(II) sorption on AM-11 and AM-14.

Kinetic Model	Fitted parameters of AM-11			R^2	R^2_{adj}	$AARD$	AIC
PFO	$q_{e\text{Exp}}$ (mg g^{-1})	$q_{e\text{Adj}}$ (mg g^{-1})	k_1(h^{-1})				
6.50 mg	150	1419	0.291	0.916	0.902	16.5	98.7
14.0 mg	70.5	70.1	0.526	0.940	0.930	15.1	69.6
PSO	$q_{e\text{Exp}}$ (mg g^{-1})	$q_{e\text{Adj}}$ (mg g^{-1})	k_2(g·mg^{-1}·h^{-1})				
6.50 mg	150	142	0.00420	0.951	0.943	9.93	87.5
14.0 mg	70.5	71.0	0.0118	0.977	0.973	9.44	55.9
Elovich		α (mg g^{-1} h^{-1})	β (g mg^{-1})				
6.50 mg		176	0.0453	0.987	0.985	4.17	67.6
14.0 mg		198	0.108	0.972	0.967	7.70	71.7
Kinetic Model	Fitted parameters of AM-14			R^2	R^2_{adj}	$AARD$	AIC
PFO	$q_{e\text{Exp}}$ (mg g^{-1})	$q_{e\text{Adj}}$ (mg g^{-1})	k_1(h^{-1})				
6.50 mg	148	146	0.223	0.949	0.941	19.8	84.9
3.50 mg	239	239	0.187	0.970	0.964	13.9	87.0
PSO	$q_{e\text{Exp}}$ (mg g^{-1})	$q_{e\text{Adj}}$ (mg g^{-1})	k_2(g·mg^{-1}·h^{-1})				
6.50 mg	148	152	0.0017	0.960	0.953	14.3	76.2
3.50 mg	239	246	0.0010	0.993	0.992	6.97	59.9
Elovich		α (mg g^{-1} h^{-1})	β (g mg^{-1})				
6.50 mg		114	0.0422	0.990	0.988	5.21	52.7
3.50 mg		104	0.0212	0.974	0.969	7.48	80.7

With respect to the calculated results achieved by the Nernst-Plank based model and the corresponding intraparticle diffusivities of counter ions, the following points can be highlighted: (i) AARD = 16.9 % for AM-11 and AARD = 10.1 % for AM-14. These are good results taking into account that the two curves for the same material were fitted simultaneously with only two parameters. (ii) The self-diffusivity of Hg(II) was 2.561×10^{-19} m^2 s^{-1} for AM-11 and 3.342×10^{-19} m^2 s^{-1} for AM-14. These values can be directly ascribed to the larger pore diameter of AM-14 (6.8 Å) in comparison with AM-11 (4 Å). (iii) The self-diffusivity of the counter ion of AM-11 (NH_4^+) was 4.593×10^{-19} m^2 s^{-1}, while for AM-14 (Na^+) it was 1.480×10^{-18} m^2 s^{-1}. The faster kinetics found in the case of AM-14 dues to the combined action of two positive effects, namely, the larger pore size of this solid and the smaller diameter of Na^+ (in opposition to NH_4^+). (IV) Finally, the estimated convective mass transfer coefficients were k_f(AM-11) = 8.5×10^{-4} m s^{-1} and k_f(AM-14) = 2.5×10^{-3} m s^{-1}.

The properly understanding about the ion exchange systems involves a good description of the equilibrium behaviour. The analysis of the isotherm curves allows to find out the best equation for design purposes, and their parameters unveil information about the surface characteristics and metal-sorbent affinity [40,61]. The main two-parameter and three-parameter isotherms are plotted for AM-11 and AM-14 in Figure 6, together with the experimental data. Both materials display favourable isotherms, and the uptake ability increases until it reaches a saturation *plateau* for AM-11, which establishes the capacity of this material. However, the same behaviour cannot be observed for AM-14 since the uptake continues to improve along the range of tested conditions. Agreeing with the Giles classification [62], which divides all isotherms into four main classes according with their initial slope and curve trend – S, L ("Langmuir"), H ("high affinity") and C ("constant partition") – the ion exchange of Hg(II) by AM-11 follows the H-type curve pattern while in the case of AM-14 it seems to follows the L-type. In the L-type isotherm the initial curvature shows that as more sites in the AM-14 are filled it becomes increasingly difficult for Hg(II) to find a vacant site available [62]. The H-type is

considered a special case of the L-type curve, in which the initial part of the isotherm is vertical due to the high affinity of the solute by the sorbent. Hence, in dilute solutions the solute tends to be completely sorbed, or at least there is no measurable amount remaining in solution [62].

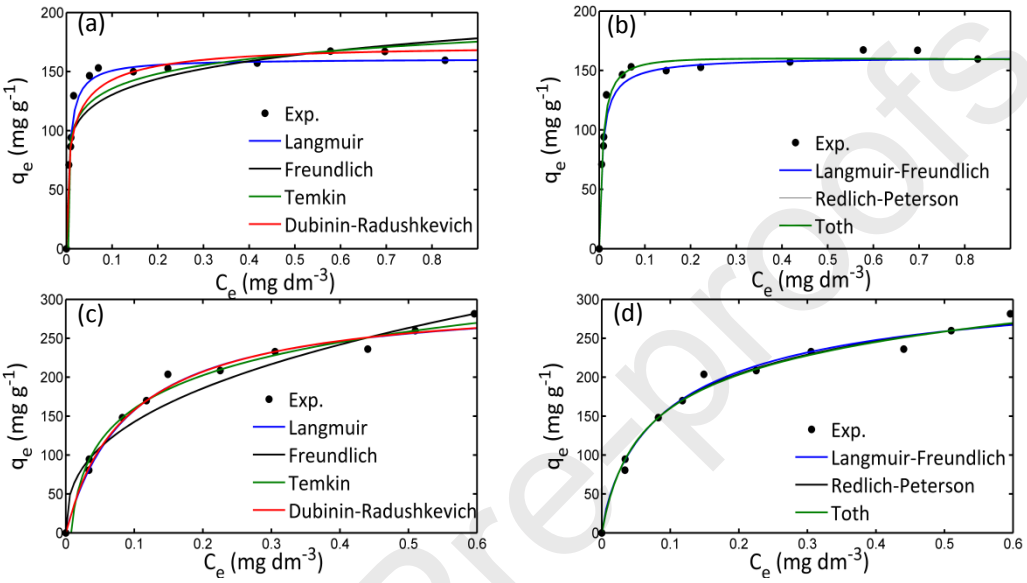

Figure 6. Sorption equilibrium isotherms on the AM-11((a) two parameters and (b) three parameters) and AM-14 ((c) two parameters and (d) three parameters).

The optimized parameters of the equilibrium models, the adjusted coefficient of determination, the average absolute relative deviations and the values of Akaike's Information Criterion are listed in Table 4 for AM-11 and in Table 5 for AM-14.

In general, the AM-11 and AM-14 equilibrium results are well described by all isotherms excluding Freundlich. According to the results obtained, the Langmuir equation describes better the Hg(II)/AM-11 system ($AARD$=3.58 %, R^2_{adj}=0.980) and the lowest AIC value observed (52.8) corroborates with this statement. The sorbent achieves a *plateau*, in accordance with the monolayer sorption characteristic of this model, and indicates an uptake capacity of 161 mg g^{-1}. The model also suggests that all active sites on the AM-11 surface possess equal affinity for Hg(II)

and constant sorption energy [40]. The mean sorption energy (E, kJ mol^{-1}) can be calculated through the Dubinin-Radushkevich parameter. The calculated value of $E = 9.91$ kJ mol^{-1} denotes the free energy change when the Hg(II) is sorbed onto the solid surface. According to Helfferich [34] as ion exchange is not a chemical reaction, the values of heat involved in the processes should be small. Normally such energy is lower than 8 kJ mol^{-1}, but values up to 40 kJ mol^{-1} have been observed in exceptional cases [34]. Therefore, it is possible to conclude that in the case of the system Hg(II)/AM-11 the removal is conducted by ion exchange. The difference between the experimental (1.60 meq g^{-1}) and theoretical (2.12 meq g^{-1}) ion exchange capacity of AM-11 suggests that some active sites may be not accessible to Hg ions.

The experimental data of the Hg(II)/AM-14 system are slightly better fitted by Temkin isotherm ($AARD$=3.92 %, R^2_{adj}=0.985, AIC=54.2), disclosing that the solid surface is more heterogeneous. Despite the measured data do not achieve an horizontal branch under the operating conditions of this study, the highest uptake observed was 280 mg g^{-1} (or 2.79 meq g^{-1}) and the capacity obtained by the Langmuir model is 304 mg g^{-1} (3.03 meq g^{-1}). Once again, the estimated value of 3.03 meq g^{-1} is inferior to the theoretical ion exchange capacity (5.20 meq g^{-1}), and the sorption energy calculated from the Dubinin-Radushkevich parameters is characteristic of an ion exchange mechanism ($E = 5.36$ kJ mol^{-1}). It is also interesting to mention a previous study performed with Hg(II)/ETS-4, for which the counter ions (Na^+ and Hg^{2+}) are the same as in AM-14, and the calculated sorption energy is quite similar, $E = 6.38$ kJ mol^{-1} [7].

Table 4 - Isotherm parameters for Hg(II) sorption on AM-11.

No. of param	Model	Fitted parameters			R^2	R^2_{adj}	$AARD$	AIC
2	Langmuir	qm_L (mg g^{-1})	K_L (dm^3 mg^{-1})					
		161	149		0.984	0.980	3.58	52.8
2	Freundlich	K_F (mg$^{1-1/nF}$ dm$^{3/nF}$ g^{-1})	n_F					
		181	7.03		0.901	0.879	9.00	76.1
2	Temkin	A (dm^3 mg^{-1})	B (mg g^{-1})					
		1.81E+04	18.1		0.922	0.905	8.07	71.6
2	Dubinin-Radushkevich	qm_{DR}(mg g^{-1})	B_{DR} (mol^2 kJ^{-2})					
		171	5.09E-09		0.953	0.942	5.65	67.6
3	Langmuir-Freundlich	qm_{LF} (mg g^{-1})	K_{LF} (dm^3 mg^{-1})^{nLF}	n_{LF}				
		162	143	0.898	0.981	0.974	3.58	60.0
3	Redlich-Peterson	K_{RP} (dm^3 g^{-1})	a_{RP} (dm^3 mg^{-1})^{nRP}	n_{RP}				
		2.26E+04	141	1.02	0.983	0.977	3.56	55.4
3	Toth	qm_{Th} (mg g^{-1})	a_{Th} (mg dm^{-3})^{nTh}	n_{Th}				
		160	3.30E-03	1.18	0.984	0.978	3.56	54.3

Table 5 - Isotherm parameters for Hg(II) sorption on AM-14.

No. of param.	Model	Fitted parameters			R^2	R^2_{adj}	$AARD$	AIC
2	Langmuir	qm_L (mg g^{-1})	K_L (dm^3 mg^{-1})					
		304	10.8		0.983	0.978	3.93	59.3
2	Freundlich	K_F (mg$^{1-1/nF}$ dm$^{3/nF}$ g^{-1})	n_F					
		343	2.63		0.968	0.959	7.11	66.6
2	Temkin	A (dm^3 mg^{-1})	B (mg g^{-1})					
		135	61.4		0.988	0.985	3.92	54.2
2	Dubinin-Radushkevich	qm_{DR}(mg g^{-1})	B_{DR} (mol^2 kJ^{-2})					
		292	1.74E-08		0.988	0.984	4.30	55.5
3	Langmuir-Freundlich	qm_{LF} (mg g^{-1})	K_{LF} (dm^3 mg^{-1})^{nLF}	n_{LF}				
		337	8.92	0.799	0.988	0.982	3.72	58.4
3	Redlich-Peterson	K_{RP} (dm^3 g^{-1})	a_{RP} (dm^3 mg^{-1})^{nRP}	n_{RP}				
		5.30E+03	16.8	0.860	0.989	0.983	3.63	58.1
3	Toth	qm_{Th} (mg g^{-1})	a_{Th} (mg dm^{-3})^{nTh}	n_{Th}				
		369	0.162	0.628	0.988	0.982	3.69	58.5

3.4. Comparison with other sorbents

In the following it is accomplished a comparison between the performance of AM-11 and AM-14 with other materials from the literature, namely: titanosilicate ETS-4; a modified zeolitic mineral of clinoptiolite-heulandite called ZNaSS; activated carbon, considered an universal adsorbent; and magnetic nanoparticles functionalized with a high Hg-affinity funtional group (dithiocarbamate). The comparison was based on the following quantities: sorbent doses used, initial mercury concentration and uptake removal (Table 6).

Table 6. Parameters related to the Hg(II) removal by various sorbents performed at temperature of 22 ℃.

Material	Sorbent doses studied (mg dm^{-3})	Hg(II) initial conc. (mg dm^{-3})	pH	q_{max} (mg g^{-1})	Reference
ETS-4	0.290-8.11	5.00E-02	4.00-5.00	246	[7]
ZNaSS **	1.00E+04	6.20-62.2	3.00	10.1	[63]
Activated Carbon *	1.50E+03	20.0	5.50	43.9	[64]
Dithiocarbamate grafted on Fe_3O_4 particles	0.248-6.13	5.00E-02	7.00	142	[53]
AM-11	1.00-14.0	1.00	6.00	161	This study
AM-14	1.50-12.0	1.00	6.00	304	This study

(*) Experiment carried out at 30 ℃. (**) No information available about temperature.

Satisfactory Hg(II) removals are reported in various works. For example, ETS-4 [7] showed a removal capacity of 246.3 mg g^{-1} and the dithiocarbamate grafted on magnetite particles [53] presented an uptake capacity of 142.0 mg g^{-1} under the same initial Hg(II) concentration of 50 μg dm^{-3}. The sorption experiments using ZNaSS [63] and activated carbon [64] were carried out under higher initial Hg(II) concentrations, in the range of 6.20-62.2 mg dm^{-3} for ZNaSS and 20.0 mg dm^{-3} for activated carbon, and the capacities reported for these materials are 10.1 and 13.3 mg g^{-1} respectively. The uptake capacities ($q_{\mathrm{m,L}}$) found for the microporous materials AM-11 (161 mg g^{-1}) and AM-14 (304 mg g^{-1}) were comparable and even higher than

the other selected materials (Table 6). These values were obtained using very low exhanger doses and highlight the great capacity of AM-14 and AM-11. The use of small quantities of AM-n materials is an advantage to treat a large volume of water, since small packed beds or stirred vessels are necessary to meet design specifications.

4. Conclusions

The sorption ability of AM-11 and AM-14 towards Hg(II) was investigated carrying out batch stirred tank experiments. Even small masses of those sorbents are able to achieve trace final concentrations of mercury. The Hg(II) removal increased with increasing contact time and mass, being possible to distinguish a fast removal in the first 48 h followed by a slower removal towards the equilibrium. PSO and Elovich models are adequated to describe the ion exchange kinetics of both materials. The values of the rate constants found (k_1, k_2 and β) agree with the mass trend, *i.e*. higher initial rates for higher masses and *vice-versa*.

The Langmuir isotherm provides the best fit to the Hg(II)/AM-11 data, predicting a sorption capacity of 161 mg g^{-1} at room temperature and pH 6 (typical of various industrial effluents and other wastewaters). The experimental data of Hg(II)/AM-14 is slightly better fitted by Temkin model and despite the full capacity of the material was not attained under the conditions studied, the highest uptake observed was 280 mg g^{-1} and the maximum uptake predicted by Langmuir model is 304 mg g^{-1}. The low mean sorption energies calculated on the basis of Dubinin-Radushkevich equation indicate that ion exchange is the mechanism for Hg(II) removal by AM-11 and AM-14. For both systems, the theoretical exchange capacity is not achieved, which may suggest that some sites are not accessible to Hg(II) ions. The performance of these two microporous niobium and vanadium silicates to uptake Hg(II) from aqueous solutions was generally excellent in comparison with other sorbents published in the literature, emphasising its high potential as ion exchangers for wastewaters treatments.

Acknowledgements

The current work has been performed with the support of CNPq *(Conselho Nacional de Desenvolvimento Científico e Tecnológico,* Brazil*)* and was developed in the scope of the project CICECO-Aveiro Institute of Materials (POCI-01-0145-FEDER-007679 | Ref. FCT UID/CTM/50011/2013) financed by national funds through the FCT/MEC and co-financed by FEDER under the PT2020 Partnership Agreement. This work was also funded by national funds (OE), through FCT – Fundação para a Ciência e a Tecnologia, I.P., in the scope of the framework contract foreseen in the numbers 4, 5 and 6 of the article 23, of the Decree-Law 57/2016, of August 29, changed by Law 57/2017, of July 19

REFERENCES

[1] R.N. Sousa, M.M. Veiga, B. Klein, K. Telmer, A.J. Gunson, L. Bernaudat, Strategies for reducing the environmental impact of reprocessing mercury-contaminated tailings in the artisanal and small-scale gold mining sector: insights from Tapajos River Basin, Brazil, J. Clean. Prod. 18 (2010) 1757–1766. doi:10.1016/J.JCLEPRO.2010.06.016.

[2] A.K. Meena, G.K. Mishra, P.K. Rai, C. Rajagopal, P.N. Nagar, Removal of heavy metal ions from aqueous solutions using carbon aerogel as an adsorbent, J. Hazard. Mater. 122 (2005) 161–170. doi:10.1016/J.JHAZMAT.2005.03.024.

[3] C. Liu, J. Peng, L. Zhang, S. Wang, S. Ju, C. Liu, Mercury adsorption from aqueous solution by regenerated activated carbon produced from depleted mercury-containing catalyst by microwave-assisted decontamination, J. Clean. Prod. 196 (2018) 109–121. doi:10.1016/J.JCLEPRO.2018.06.027.

[4] Substance Priority List | ATSDR, (2017). https://www.atsdr.cdc.gov/spl/ (accessed February 2, 2019).

[5] C. Qi, X. Ma, M. Wang, L. Ye, Y. Yang, J. Hong, A case study on the life cycle assessment of recycling industrial mercury-containing waste, J. Clean. Prod. 161 (2017) 382–389. doi:10.1016/J.JCLEPRO.2017.05.023.

[6] C.B. Lopes, P.F. Lito, M. Otero, Z. Lin, J. Rocha, C.M. Silva, E. Pereira, A.C. Duarte, Mercury removal with titanosilicate ETS - 4 : Batch experiments and modelling, Microporous Mesoporous Mater. 115 (2008) 98–105. doi:10.1016/j.micromeso.2007.10.055.

[7] C.B. Lopes, M. Otero, Z. Lin, C.M. Silva, J. Rocha, E. Pereira, A.C. Duarte, Removal of Hg2+ ions from aqueous solution by ETS-4 microporous titanosilicate-Kinetic and equilibrium studies, Chem. Eng. J. 151 (2009) 247–254. doi:10.1016/j.cej.2009.02.035.

[8] A. Johs, V.A. Eller, T.L. Mehlhorn, S.C. Brooks, D.P. Harper, M.A. Mayes, E.M. Pierce, M.J. Peterson, Dissolved organic matter reduces the effectiveness of sorbents for mercury removal, Sci. Total Environ. 690 (2019) 410–416. doi:10.1016/j.scitotenv.2019.07.001.

[9] W. Dong, L. Liang, S. Brooks, G. Southworth, B. Gu, Roles of dissolved organic matter in the speciation of mercury and methylmercury in a contaminated ecosystem in Oak Ridge, Tennessee, Environ. Chem. 7 (2010) 94–102. doi:10.1071/EN09091.

[10] S.S. Baral, N. Das, T.S. Ramulu, S.K. Sahoo, S.N. Das, G.R. Chaudhury, Removal of Cr(VI) by thermally activated weed Salvinia cucullata in a fixed-bed column, J. Hazard. Mater. 161 (2009) 1427–1435. doi:10.1016/j.jhazmat.2008.04.127.

[11] C.B. Lopes, P.F. Lito, S.P. Cardoso, E. Pereira, A.C. Duarte, C.M. Silva, Metal recovery, separation and/or pre-concentration, in: Inamuddin, M. Luqma (Eds.), Ion Exch. Technol. II – Appl., Springer, 2012: pp. 237–322.

[12] L.D. Barreira, P.F. Lito, B.M. Antunes, M. Otero, Z. Lin, J. Rocha, E. Pereira, A.C. Duarte, C.M. Silva, Effect of pH on cadmium (II) removal from aqueous solution using titanosilicate ETS-4, Chem. Eng. J. 155 (2009) 728–735.

[13] Ihsanullah, A. Abbas, A.M. Al-Amer, T. Laoui, M.J. Al-Marri, M.S. Nasser, M. Khraisheh, M.A. Atieh, Heavy metal removal from aqueous solution by advanced carbon nanotubes: Critical review of adsorption applications, Sep. Purif. Technol. 157 (2016) 141–161. doi:10.1016/j.seppur.2015.11.039.

[14] Y. Huang, D. Wu, X. Wang, W. Huang, D. Lawless, X. Feng, Removal of heavy metals from water using polyvinylamine by polymer-enhanced ultrafiltration and flocculation, Sep. Purif. Technol. 158 (2016) 124–136. doi:10.1016/j.seppur.2015.12.008.

[15] M. Sajid, M.K. Nazal, Ihsanullah, N. Baig, A.M. Osman, Removal of heavy metals and

organic pollutants from water using dendritic polymers based adsorbents: A critical review, Sep. Purif. Technol. 191 (2018) 400–423. doi:10.1016/j.seppur.2017.09.011.

[16] Ihsanullah, Carbon nanotube membranes for water purification: Developments, challenges, and prospects for the future, Sep. Purif. Technol. 209 (2019) 307–337. doi:https://doi.org/10.1016/j.seppur.2018.07.043.

[17] A. Bhatnagar, M. Sillanpää, A. Witek-Krowiak, Agricultural waste peels as versatile biomass for water purification - A review, Chem. Eng. J. 270 (2015) 244–271. doi:10.1016/j.cej.2015.01.135.

[18] A. Dąbrowski, Z. Hubicki, P. Podkościelny, E. Robens, Selective removal of the heavy metal ions from waters and industrial wastewaters by ion-exchange method, Chemosphere. 56 (2004) 91–106. doi:10.1016/j.chemosphere.2004.03.006.

[19] E.D. Camarinha, P.F. Lito, B.M. Antunes, M. Otero, Z. Lin, J. Rocha, E. Pereira, A.C. Duarte, C.M. Silva, Cadmium(II) removal from aqueous solution using microporous titanosilicate ETS-10, Chem. Eng. J. 155 (2009) 108–114. doi:10.1016/j.cej.2009.07.015.

[20] S. Wierzba, A. Kłos, Heavy metal sorption in biosorbents – Using spent grain from the brewing industry, J. Clean. Prod. 225 (2019) 112–120. doi:10.1016/J.JCLEPRO.2019.03.286.

[21] D. Czarna, P. Baran, P. Kunecki, R. Panek, R. Żmuda, M. Wdowin, Synthetic zeolites as potential sorbents of mercury from wastewater occurring during wet FGD processes of flue gas, J. Clean. Prod. 172 (2018) 2636–2645. doi:10.1016/J.JCLEPRO.2017.11.147.

[22] S. Ahmed, S. Chughtai, M.A. Keane, The removal of cadmium and lead from aqueous solution by ion exchange with Na-Y zeolite, Sep. Purif. Technol. 13 (1998) 57–64. doi:10.1016/S1383-5866(97)00063-4.

[23] S. Araki, T. Li, K. Li, H. Yamamoto, Preparation of zeolite hollow fibers for high-efficiency cadmium removal from waste water, Sep. Purif. Technol. 221 (2019) 393–398. doi:10.1016/j.seppur.2019.04.011.

[24] B. Biškup, B. Subotić, Kinetic analysis of the exchange processes between sodium ions from zeolite A and cadmium, copper and nickel ions from solutions, Sep. Purif. Technol. 37 (2004) 17–31. doi:10.1016/S1383-5866(03)00220-X.

[25] P.F. Lito, S.P. Cardoso, J.M. Loureiro, C.M. Silva, Ion Exchange Equilibria and Kinetics, in: Inamuddin, M. Luqman (Eds.), Ion Exch. Technol. I – Appl., Springer, 2012: pp. 51–120.

[26] Y.D. Noh, S. Komarneni, K.J.D. MacKenzie, Titanosilicates: Giant exchange capacity and selectivity for Sr and Ba, Sep. Purif. Technol. 95 (2012) 222–226. doi:10.1016/j.seppur.2012.05.013.

[27] S.P. Cardoso, C.B. Lopes, E. Pereira, A.C. Duarte, C.M. Silva, Competitive Removal of Cd2+ and Hg2+ Ions from Water Using Titanosilicate ETS-4: Kinetic Behaviour and Selectivity, Water, Air, Soil Pollut. 224 (2013) 1535. doi:10.1007/s11270-013-1535-z.

[28] T.R. Ferreira, C.B. Lopes, P.F. Lito, M. Otero, Z. Lin, J. Rocha, E. Pereira, C.M. Silva, A. Duarte, Cadmium(II) removal from aqueous solution using microporous titanosilicate ETS-4, Chem. Eng. J. 147 (2009) 173–179. doi:10.1016/j.cej.2008.06.032.

[29] J. Rocha, P. Brandao, A. Phillippou, M.W. Anderson, Synthesis and characterisation of a novel microporous niobium silicate catalyst, Chem Commun. (1998) 2687–2688. doi:Doi 10.1039/A808264b.

[30] P. Brandão, A. Philippou, N. Hanif, P. Ribeiro-Claro, A. Ferreira, M.W. Anderson, J. Rocha, Synthesis and characterization of two novel large-pore crystalline vanadosilicates, Chem. Mater. 14 (2002) 1053–1057. doi:10.1021/cm010613q.

[31] P. Brandão, A. Philippou, J. Rocha, M.W. Anderson, Dehydration of alcohols by microporous niobium silicate AM-11, Catal. Letters. 80 (2002) 99–102. doi:10.1023/A:1015444005961.

[32] C.B. Lopes, J. Coimbra, M. Otero, E. Pereira, A.C. Duarte, Z. Lin, J. Rocha, Uptake of Hg2+ from aqueous solutions by microporous titano- and zircono-silicates, Quim. Nov. 31 (2008) 321–325. http://www.scielo.br/pdf/qn/v31n2/a25v31n2.pdf (accessed March 26, 2018).

[33] S. Azizian, Kinetic models of sorption: a theoretical analysis, J. Colloid Interface Sci. 276 (2004) 47–52. doi:10.1016/j.jcis.2004.03.048.

[34] F.G. Helfferich, Ion Exchange, McGraw-Hill, New York, 1962.

[35] A.E. Rodrigues, C.M. Silva, What's wrong with Lagergreen pseudo first order model for adsorption kinetics?, Chem. Eng. J. 306 (2016) 1138–1142. doi:10.1016/j.cej.2016.08.055.

[36] S. Lagergren, Zur theorie der sogenannten adsorption gel Zur theorie der sogenannten adsorption gelster stoffe, Kungliga Svenska Vetenskapsakademiens, Handlingar. 24 (1898) 1–39.

[37] Z. Aksu, Application of biosorption for the removal of organic pollutants: a review, Process Biochem. 40 (2005) 997–1026. doi:10.1016/j.procbio.2004.04.008.

[38] Y.S. Ho, G. McKay, Pseudo-second order model for sorption processes, Process Biochem. 34 (1999) 451–465. doi:10.1016/S0032-9592(98)00112-5.

[39] S. Roginsky, Y.B. Zeldovich, The catalytic oxidation of carbon monoxide on manganese dioxide, Acta Phys. Chem. USSR. 1 (1934) 554.

[40] Y.S. Ho, J.F. Porter, G. Mckay, Equilibrium isotherm studies for the sorption of divalentmetal ions onto peat: copper, nickel and lead single component systems, Water, Air, Soil Pollut. 141 (2002) 1–33. doi:10.1023/A:1021304828010.

[41] I. Langmuir, The adsorption of gases on plane surface of glass, mica and platinum, J.Am, Chem.Soc. 40 (1916) 1361–1368.

[42] A.. Dada, A.. Olalekan, A.. Olatunya, O. Dada, Langmuir , Freundlich , Temkin and Dubinin – Radushkevich Isotherms Studies of Equilibrium Sorption of Zn 2 + Unto Phosphoric Acid Modified Rice Husk, IOSR J. Appl. Chem. 3 (2012) 38–45. doi:10.9790/5736-0313845.

[43] H. Freundlich, Concerning adsorption in solutions., Zeitschrift Fur Phys. Chemie-Stochiometrie Und Verwandstchaftslehre. 57 (1906) 385–470.

[44] D.D. Do, Adsorption analysis: equilibria and kinetics, Imperial College Press, London, 1998.

[45] A. Bourane, M. Nawdali, D. Bianchi, Heats of Adsorption of the Linear CO Species Adsorbed on a Ir/Al 2 O 3 Catalyst Using in Situ FTIR Spectroscopy under Adsorption Equilibrium, J. Phys. Chem. B. 106 (2002) 2665–2671. doi:10.1021/jp0137322.

[46] M. Polanyi, Adsorption from the point of view of the Third Law of Thermodynamics, Verh. Deut. Phys. Ges. 16 (1914) 1012–1016.

[47] M.M. Dubinin, The Potential Theory of Adsorption of Gases and Vapors for Adsorbents with Energetically Nonuniform Surfaces., Chem. Rev. 60 (1960) 235–241. doi:10.1021/cr60204a006.

[48] V.J. Inglezakis, Solubility-normalized Dubinin–Astakhov adsorption isotherm for ion-exchange systems, Microporous Mesoporous Mater. 103 (2007) 72–81. doi:10.1016/J.MICROMESO.2007.01.039.

[49] S.P. Cardoso, I.S. Azenha, I. Portugal, Z. Lin, A.E. Rodrigues, C.M. Silva, Single and binary surface diffusion permeation through zeolite membranes using new Maxwell-Stefan factors for Dubinin-type isotherms and occupancy-dependent kinetics, Sep. Purif. Technol. 182 (2017) 207–218. doi:10.1016/j.seppur.2017.03.036.

[50] B. Smit, T. Maesen, Molecular simulations of zeolites : Adsorption , diffusion , and shape selectivity, Chem. Rev. 108 (2008) 4125–4184. doi:10.1021/cr8002642.

[51] S. Ali Khan, Riaz-ur-Rehman, M. Ali Khan, Sorption of cesium on bentonite, Waste Manag. 14 (1994) 629–642. doi:10.1016/0956-053X(94)90035-3.

[52] M. Rashid, F. Khan, Lutfullah, Removal of Pb(II) ions from aqueous solutions using hybrid organic–inorganic composite material: Zr(IV) iodosulphosalicylate, J. Water Process Eng. 3 (2014) 53–61. doi:10.1016/J.JWPE.2014.07.003.

[53] P. Figueira, C.B. Lopes, A.L. Daniel-da-Silva, E. Pereira, A.C. Duarte, T. Trindade, Removal of mercury (II) by dithiocarbamate surface functionalized magnetite particles: application to synthetic and natural spiked waters., Water Res. 45 (2011) 5773–5784. doi:10.1016/j.watres.2011.08.057.

[54] R.J. Umpleby, S.C. Baxter, Y. Chen, R.N. Shah, K.D. Shimizu, Characterization of molecularly imprinted polymers with the Langmuir-Freundlich isotherm., Anal. Chem. 73 (2001) 4584–91. http://www.ncbi.nlm.nih.gov/pubmed/11605834 (accessed March 28, 2017).

[55] S.J. Allen, G. Mckay, J.F. Porter, Adsorption isotherm models for basic dye adsorption by peat in single and binary component systems, J. Colloid Interface Sci. 280 (2004) 322–333. doi:10.1016/J.JCIS.2004.08.078.

[56] G.F. Malash, M.I. El-Khaiary, Piecewise linear regression: A statistical method for the analysis of experimental adsorption data by the intraparticle-diffusion models, Chem. Eng. J. 163 (2010) 256–263. doi:10.1016/j.cej.2010.07.059.

[57] E. Fabre, C. Vale, E. Pereira, C.M. Silva, Experimental Measurement and Modeling of Hg(II) Removal from Aqueous Solutions Using Eucalyptus globulus Bark: Effect of pH, Salinity and Biosorbent Dosage, Int. J. Mol. Sci. 20 (2019) 5973. doi:10.3390/ijms20235973.

[58] L. Carro, V. Anagnostopoulos, P. Lodeiro, J.L. Barriada, R. Herrero, M.E. Sastre de Vicente, A dynamic proof of mercury elimination from solution through a combined

sorption–reduction process, Bioresour. Technol. 101 (2010) 8969–8974. doi:10.1016/J.BIORTECH.2010.06.118.

[59] R. Herrero, P. Lodeiro, C. Rey-Castro, T. Vilariño, M.E. Sastre De Vicente, Removal of inorganic mercury from aqueous solutions by biomass of the marine macroalga Cystoseira baccata, Water Res. 39 (2005) 3199–3210. doi:10.1016/j.watres.2005.05.041.

[60] N. Zandi-Atashbar, A.A. Ensafi, A.H. Ahoor, Magnetic Fe2CuO4/rGO nanocomposite as an efficient recyclable catalyst to convert discard tire into diesel fuel and as an effective mercury adsorbent from wastewater, J. Clean. Prod. 172 (2018) 68–80. doi:10.1016/J.JCLEPRO.2017.10.146.

[61] A. Maleki, Z. Hajizadeh, V. Sharifi, Z. Emdadi, A green, porous and eco-friendly magnetic geopolymer adsorbent for heavy metals removal from aqueous solutions, J. Clean. Prod. 215 (2019) 1233–1245. doi:10.1016/j.jclepro.2019.01.084.

[62] C.. Giles, T.. MacEwan, S.. Nakhwa, D. Smith, Studies in adsorption. Part XI. A system of classification of solution adsorption isotherms, and its use in diagnosis of adsorption mechanisms and in measurement of specific surface areas of solids, J. Chem. Soc. 786 (1960) 3973–3993. doi:10.1016/S0008-6223(03)00002-2.

[63] T. Gebremedhin-Haile, M.T. Olguín, M. Solache-Ríos, Removal of mercury ions from mixed aqueous metal solutions by natural and modified zeolitic minerals, Water. Air. Soil Pollut. 148 (2003) 179–200.

[64] K. Ranganathan, Adsorption of Hg(II) ions from aqueous chloride solutions using powdered activated carbons, Carbon N. Y. 41 (2003) 1087–1092. doi:10.1016/S0008-6223(03)00002-2.

[65] N. Fiol, I. Villaescusa, Determination of sorbent point zero charge: usefulness in sorption studies, Environ. Chem. Lett. 7 (2009) 79–84.

[66] S.P. Cardoso, I.S. Azenha, Z. Lin, I. Portugal, A.E. Rodrigues, C.M. Silva. Experimental measurement and modeling of ion exchange equilibrium and kinetics of cadmium(II) solutions over microporous stannosilicate AV-6, Chem. Eng. J. 295 (2016) 139-151.

[67] P.F. Lito, J.P.S. Aniceto, C.M. Silva, Maxwell–Stefan based modelling of ion exchange systems containing common species (Cd^{2+}, Na^{+}) and distinct sorbents (ETS-4, ETS-10), Int. J. Environ. Sci. Technol. 12 (2013) 183–192.

[68] C.B. Lopes, E. Pereira, Z. Lin, P. Pato, M. Otero, C.M. Silva, J. Rocha, A.C. Duarte. Fixed-bed removal of Hg2+from contaminated water by microporous titanosilicate ETS-4: Experimental and theoretical breakthrough curves, *Microp. Mesop. Mat.* 145 (2011) 32-40.

[69] M. Otero, C.B. Lopes, J. Coimbra, T.R. Ferreira, C.M. Silva, Z. Lin, J. Rocha, E. Pereira, A.C. Duarte. Priority pollutants (Hg2+and Cd2+) removal from water by ETS-4 titanosilicate, Desalination 249 (2009) 742-747.

[70] E. Fabre, C.B. Lopes, C. Vale, E. Pereira, C.M. Silva, Valuation of banana peels as an effective biosorbent for mercury removal under low environmental concentrations, Sci. Total Environ. (2019). doi:DOI: 10.1016/j.scitotenv.2019.135883.

[71] R. Melamed, A.B. da Luz, Efficiency of industrial minerals on the removal of mercury species from liquid effluents, Sci. Total Environ. 368 (2006) 403–406.

[72] H. Javadian, M. Taghavi, Application of novel Polypyrrole/thiol-functionalized zeolite Beta/MCM-41 type mesoporous silica nanocomposite for adsorption of Hg 2+ from aqueous solution and industrial wastewater: Kinetic, isotherm and thermodynamic studies, Appl. Surf. Sci. 289 (2014) 487–494.

Highlights

- Niobium and vanadium microporous silicates exhibit extraordinary ion exchange properties
- AM-11 and AM-14 silicates were tested for mercury(II) removal from contaminated water
- Kinetic and equilibrium experiments were performed and accurately modeled
- Pseudo-second order and Elovich models were able to represent the purification kinetics
- Ion exchange capacity from Langmuir model: 161 mg g^{-1} (AM-11) and 304 mg g^{-1} (AM-14)

Authors Statement

Elaine Fabre: Writing - original draft; Investigation; Methodology

Arany Rocha: Writing - original draft; Investigation; Methodology

Simão P. Cardoso: Investigation; Methodology

Paula Brandão: Methodology; Resources

Carlos Vale: Writing - review & editing; Formal analysis

Cláudia B. Lopes: Investigation; Methodology; Formal analysis

Eduarda Pereira: Funding acquisition; Supervision; Writing - review & editing; Resources

Carlos M. Silva: Funding acquisition; Supervision; Writing - review & editing; Conceptualization; Resources; Formal analysis

Declaration of interests

The authors declare that they have no known competing financial interests or personal relationships that could have appeared to influence the work reported in this paper.

Carlos Manuel Silva

(Corresponding Author, on behalf of all coauthors)